Am J Physiol Heart Circ Physiol 282: H1534–H1547, 2002.
First published November 29, 2001; 10.1152/ajpheart.00351.2001.

Mathematical analysis of dynamics of cardiac memory and accommodation: theory and experiment

MARI A. WATANABE[1,2] AND MARCUS L. KOLLER[3]
[1]*Institute of Biomedical and Life Sciences, Glasgow University, Glasgow G12 8QQ, United Kingdom;* [2]*Center for Interdisciplinary and Complex Systems, Northeastern University, Boston, Massachusetts 02115; and* [3]*Medizinische Klinik der Universität Würzburg, 97080 Würzburg, Germany*

Received 27 April 2001; accepted in final form 19 November 2001

Watanabe, Mari A., and Marcus L. Koller. Mathematical analysis of dynamics of cardiac memory and accommodation: theory and experiment. *Am J Physiol Heart Circ Physiol* 282: H1534–H1547, 2002. First published November 29, 2001; 10.1152/ajpheart.00351.2001.—Decreasing the slope of the dynamic, but not conventional, restitution curves is antifibrillatory. Cardiac memory/accommodation underlies the difference. We measured diastolic interval (DI) and action potential duration (APD) in epicardial, endocardial, and Purkinje tissue from eight dogs. Consecutive 100-stimulus trains were given to study transitions between basic cycle lengths (BCL) ranging from 400 to 1,300 ms. (DI,APD) pairs aligned immediately on the line DI + APD = BCL (64/67) or oscillated (3/67). The shifting effect of up to 10 extrastimuli on restitution curves was also measured. These curves were fit with the equation $APD = \alpha + \beta \exp(-DI/\tau)$, where α is asymptote, β is drop, and τ is time constant. Linear regression of the parameters against the number of extrastimuli showed that premature and postmature stimuli decreased and increased α and β and increased and decreased τ, respectively. Analysis of a mathematical model treating memory as an exponentially decreasing shift of restitution curves shows that oscillatory DI,APD is expected with large ΔBCL, steep restitution slope, or increased cardiac accommodation. The model explains phase shifts and suggests a common mechanism for Purkinje and myocardial electrical alternans.

arrhythmias; dynamic restitution; short-term memory; modeling

SUDDEN CARDIAC DEATH claims over 300,000 lives in the United States each year (53) despite the invention of the implantable cardiac defibrillator and improvement in antiarrhythmic drugs. A better understanding of the mechanisms of ventricular tachyarrhythmias is still needed for prediction and treatment of sudden cardiac death. Modeling studies predict that a steeply (>1) sloped action potential duration (APD) restitution curve should produce breakup of spiral waves into ventricular fibrillation, whereas a shallow slope should prevent ventricular fibrillation (23, 36, 37). Studies from patients with coronary artery disease (9, 52), and some animal studies (25, 51) show that the maximum slope of the restitution curve can be much less than 1. If that were always true, ventricular fibrillation would never occur. A recent experiment designed to study this paradox demonstrated that the slope of the "dynamic" restitution curve, which is the relationship between APD and preceding diastolic interval (DI) measured during rapid pacing or during ventricular fibrillation, has a slope greater than that measured by the standard S1S2 protocol (25). The slope of the dynamic restitution curve has also been found to correlate with tachycardia stability. For example, verapamil, which was observed to convert ventricular fibrillation to ventricular tachycardia experimentally (49, 44), decreases the slope of the dynamic restitution curve, whereas procainamide, which decreases the slope of the standard restitution curve, has no effect on ventricular fibrillation (39). The difference between the two types of restitution curves is due to cardiac memory. Cardiac memory increases the effective slope of the restitution function (15). It has also been shown that spiral wave breakup can be induced in a mathematical model with flat standard restitution curves if memory is included (10). These results point to a critical role for cardiac memory in the stability and perpetuation of ventricular arrhythmias.

However, cardiac memory has not been measured systematically for several reasons. First, memory implies that the entire past activation history of cardiac tissue determines a single APD of interest. It is difficult to quantify history by a single value. In contrast, APD dependence on preceding DI, i.e., restitution, is easily quantified by varying the coupling interval of a premature stimulus. Second, the significance of cardiac memory in arrhythmogenesis had been equivocal until the recent studies of dynamic restitution. Third, for most of the history of cardiac electrophysiology APD was measured manually, and the laborious nature of this task limited the number of APDs that could be measured. The goal of this study was to explore methods for quantifying and characterizing cardiac memory in concrete ways. The model of cardiac memory we present is based on the concept that memory is the amount by which restitution curves are shifted with

Address for reprint requests and other correspondence: M. A. Watanabe, Inst. of Biomedical and Life Sciences, West Medical Bldg., Univ. of Glasgow, Glasgow G12 8QQ, UK (E-mail: mwata001@udcf.gla.ac.uk).

The costs of publication of this article were defrayed in part by the payment of page charges. The article must therefore be hereby marked "*advertisement*" in accordance with 18 U.S.C. Section 1734 solely to indicate this fact.

stimulus basic cycle length change (ΔBCL). The model produces clear predictions about the dynamic behavior of APD after a cycle length change and is able to reproduce our experimental results as well as explain several phenomena seen in the literature.

MATERIALS AND METHODS

Experiments

Hearts were excised from eight adult beagle or mongrel dogs of either sex anesthetized with pentobarbital solution (86 mg/kg iv, Fatal-Plus; Votech Pharmaceuticals, Dearborn, MI) and placed in cool Tyrode solution (in mmol/l: 0.5 $MgCl_2$, 0.9 NaH_2PO_4, 2.0 $CaCl_2$, 137.0 NaCl, 24.0 $NaHCO_3$, 4.0 KCl, and 5.5 glucose). All experimental procedures were conducted in accordance with guidelines set by the Institutional Animal Care and Use Committee of the Center for Research Animal Resources at Cornell University. Purkinje fibers (PF; $n = 4$), strips of endocardial tissue ($n = 4$), and strips of epicardial tissue ($n = 3$) dissected from either left or right ventricle were mounted in Plexiglas chambers and superfused with 37.0°C Tyrode solution gassed with 95% O_2-5% CO_2. The tissue was stimulated by bipolar platinum wire electrodes (interelectrode distance 1 mm) at twice late diastolic threshold intensity. Transmembrane potentials recorded by conventional microelectrode technique were digitized by AcqKnowledge software (version 3.2.6; Biopac Systems) at 1,000 Hz (resolution of 1 ms) and analyzed with a program written in the MatLab language (version 5.2; MathWorks). APD and DI were measured at 95% repolarization. If stimulus coupling intervals were short and action potentials arose before full repolarization, APD value of the truncated action potential was calculated from an extrapolation of phase 3 to the baseline. APD values were rounded to the nearest integer value. Nonlinear curve fitting was performed with SigmaPlot software (version 4.11; Jandel Scientific). Linear regression and statistical analyses were performed with StatView software (version 5.0; SAS Institute). P values < 0.05 were considered to be statistically significant. Values are expressed as means ± SD unless otherwise noted.

Two stimulus protocols were used (Fig. 1). In *protocol 1*, we measured sequential DI and APD values after an abrupt change from one cycle length to another. The tissue was paced

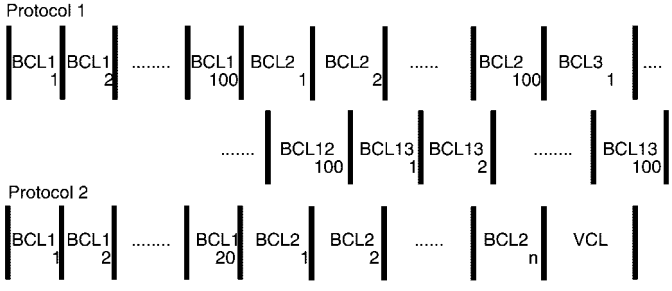

Fig. 1. Stimulus protocols used in experiments. In *protocol 1*, stimulation was given 100 times at a basic cycle length (BCL) before switching to a new BCL. Four BCL were studied: 400, 700, 1,000, and 1,300 ms. A typical sequence of BCL was 400, 1,300, 1,000, 700, 400, 1,000, 1,300, 700, 1,000, 400, 700, 1,300, and 400. Duration of every action potential was measured. In *protocol 2*, BCL1 (old BCL) and BCL2 (new BCL) were chosen from 400, 700, 1,000, or 1,300 ms. The BCL1 train always had 20 intervals. The BCL2 train ranged from 0 to 10 intervals. Finally, a stimulus was given at variable cycle length (VCL) ranging from 150 to 1,000 ms for the purpose of restitution curve measurement. n, Stimulus number.

100 times at one BCL, 100 times at a second BCL, 100 times at a third BCL, and so forth, until all 12 transitions between the 4 BCL of 400, 700, 1,000, and 1,300 ms had been covered. Each 100-stimulus train was begun synchronized to the last stimulus of the previous train. All 1,200 APDs were measured. In *protocol 2*, we measured shifts in the restitution curve produced by multiple extrastimuli. Effects of different numbers of premature stimuli on a given restitution curve were studied by inserting different numbers of premature stimuli between a train of 20 stimuli and the test stimulus given at variable coupling intervals for measuring restitution. More specifically, the tissue was given a 20-stimulus train (S1) at a BCL of 400, 700, 1,000, or 1,300 ms, an n-stimulus train (S2) at a BCL of 400, 700, 1,000, or 1,300 ms, and a final stimulus (S3) that was coupled to the last stimulus of the second train by a coupling interval (S2S3) of 150, 200, 250, 300, 400, 700, or 1,000 ms. The APD produced by the last S2 stimulus of the second train and the APD produced by the final stimulus (S3) were measured. This protocol was repeated for n of 0, 1, 2, 3, 4, 5, and 10. In both protocols, there were transitions between various pacing cycle lengths. We called the pacing cycle length before a transition "old" BCL and the one after a transition (such as the S2 train in *protocol 2*) "new" BCL. The new BCL became old BCL when the pacing cycle length was changed again. We defined ΔBCL as old BCL − new BCL, so ΔBCL was positive when the pacing rate was accelerated.

Stimulus *protocol 1* was tested in six preparations (1 epicardial, 3 endocardial, and 2 PF). Data were studied in two ways. First, the DI preceding and the APD following each stimulus were plotted as pairs in DI,APD parameter space to assess how the pairs approached the line representing the equation DI + APD = new BCL. Second, APD for each stimulus was plotted vs. stimulus number to assess how APD (100-APD sequence) evolved toward the steady-state value of the new BCL. In that analysis, APD values were fit by an exponential function of the form $APD = \alpha + \beta \exp(-\text{stimulus number}/\eta)$ with three independent parameters α, β, and η, which we called asymptote, drop, and time constant. Note that η in this protocol is not the conventional time constant measured in milliseconds but has units of stimulus number, which can be converted to time by multiplying by new BCL.

Data from stimulus *protocol 2* were studied in five preparations (2 epicardial, 1 endocardial, and 2 PF tissue). The data analysis process is best followed by referring to Fig. 2. To characterize evolution of restitution curves after different numbers of extrastimuli, we fit each restitution curve (the 7 restitution curves after 0–10 extrastimuli) with an exponential function of the form $APD = \alpha + \beta \exp(-DI/\tau)$, where τ is time constant (Fig. 2*A*). The values of a given parameter were plotted against the number of premature stimuli and fit with linear regression functions, resulting in a slope and intercept value for each of the three parameters (Fig. 2*B*). These six slope and intercept parameters were in turn plotted against new BCL, old BCL, or ΔBCL. Fig. 2*C* shows the intercept of α plotted against old BCL; Fig. 2*D* shows the slope of α against ΔBCL. These plots were themselves fit with linear regression functions. Because the slope should not have changed if BCL did not change, regression fits of the slope parameter plots were forced through the origin. A fourth parameter, δ, describing the horizontal shift of restitution curves was also computed using the formula $\tau * \ln(\beta'/\beta)$, after τ and β were obtained from the exponential regression fitting. (The asterisk symbol signifies multiplication here and hereafter.) β'/β is the ratio of β after extrastimuli to β in the absence of extrastimuli. This formula assumes a constant τ and merely reflects the fact that a vertical shift of an exponential curve is equivalent to a horizontal shift of that curve, similar to the way in which a vertical shift of a straight line ($y =$

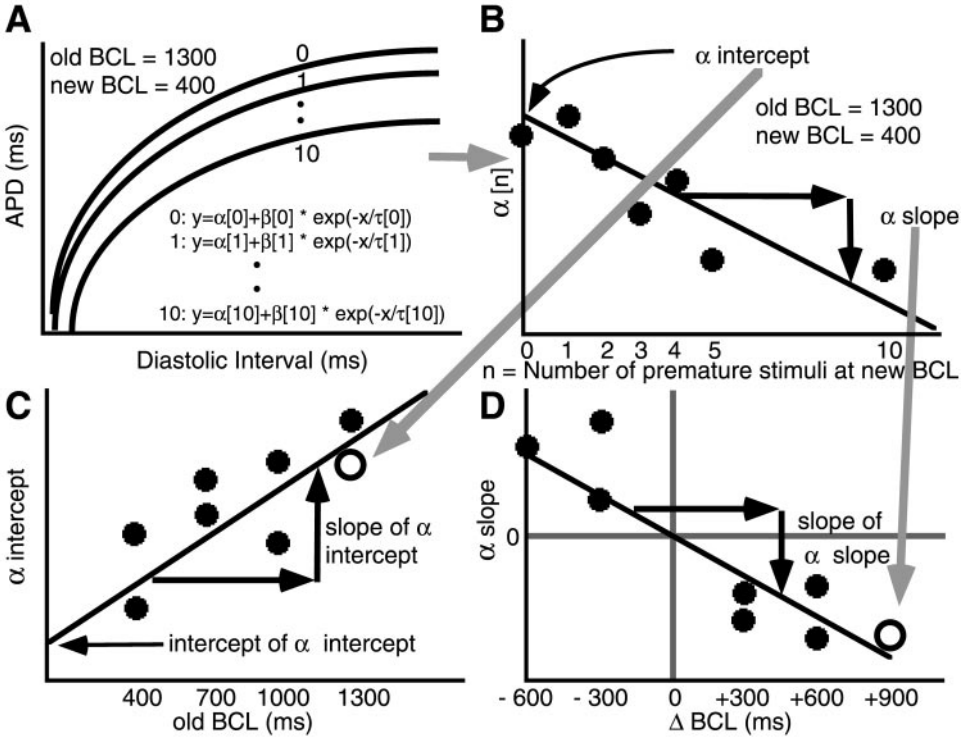

Fig. 2. Schematic diagrams showing method of analysis of restitution curve evolution data. *A*: in stimulus *protocol 2* (*Fig. 1*), 0–5 and 10 extrastimuli with coupling interval of new BCL were given after a train of 20 stimuli with coupling interval of old BCL. Restitution curves shifted with increasing numbers of extrastimuli (numbers in brackets). Each curve was fit with a monoexponential equation. *B*: the 3 independent parameters describing the exponential restitution curves were plotted against the number of extrastimuli. A schematic plot for parameter α is shown here with its linear regression curve. The linear fit produced a slope and an intercept value. *C* and *D*: the intercept and slope values found in *B* were plotted against old BCL and ΔBCL, respectively, (○) along with values found from stimulus runs that studied other combinations of old and new BCL (●). Linear regression on these data produced further slope and intercept values.

$ax + b$) by amount c ($y = ax + b - c$) is equivalent to a horizontal shift of the same line by amount c/a [$y = a(x - c/a) + b$]. Once all of the curve fitting was completed, the statistical significance of the regression lines of the slopes and intercepts on BCL parameter (new, old, ΔBCL) was determined, and if there was no significant dependence of an exponential parameter on any of the BCL parameters, the parameter was assumed fixed for a given tissue and its average value was computed.

Mathematical Model

We assumed that the restitution curve was linear, i.e., that it could be described by an equation of the form $y = a * x + b$, where y is APD and x is DI. This assumption was made to facilitate the drawing of mathematically exact conclusions but was justified on the basis of our experimental results from stimulus *protocol 1* showing rapid, nonoscillatory adaptation of DI and APD to change in cycle length, so that there was only a narrow (and in that sense, linear) segment of restitution curve explored after the first two beats in the majority of cases. Our second assumption was that an abrupt change to a new BCL produced a change in memory described by a vertical shift of restitution function of k_n ms with each new stimulus. The first shift was indexed 0 (see Fig. 3). A vertical shift of k is equivalent to a horizontal shift of k/a in a linear system, so analysis of the vertical shift case can be extrapolated to horizontal shift by constant scaling. The two assumptions gave the following iterative equations

$$y_n = a * x_n + b - K_{n-2} \quad (1)$$

$$x_{n+1} = T - y_n \quad (2)$$

where K is the cumulative shift, $K_0 = k_0$, $K_1 = k_0 + k_1$, etc., or

$$K_n = \sum_{i=0}^{n} k_i = k_0 + k_1 + k_2 + \cdots + k_n \quad (3)$$

T is the new BCL and, $K_{-1} = 0$ (see Fig. 3). The subscript n denotes the stimulus number at the new BCL, x_n is the DI preceding that stimulus, and y_n is the APD produced by that stimulus. The steady-state DI and APD values at the old BCL were x_0 and y_0, respectively. [At steady state, the restitution function is no longer shifting, and (x_0,y_0) must lie at the intersection of $x + y =$ old BCL and the steady-state restitution function at the old BCL.] We also defined the difference d_n in consecutive APD as

$$d_n = y_n - y_{n+1} \quad (4)$$

such that decreasing APD gave positive d values. From the assumptions, it was also true that

$$d_0 = (\text{old BCL} - \text{new BCL}) * a \quad (5)$$

We analyzed the dynamics of *Eq. 4* for the case of k_n described by the exponentially decreasing function

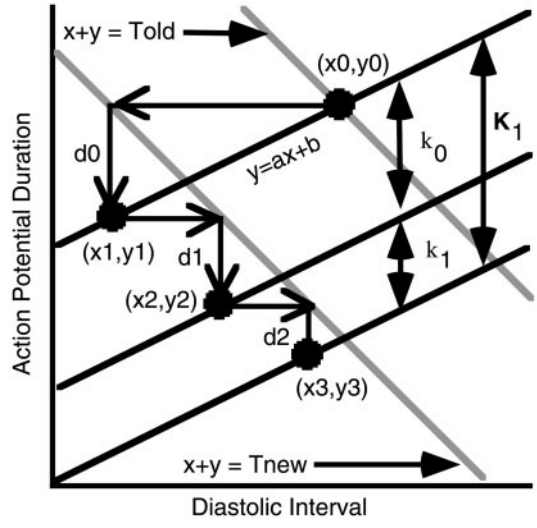

Fig. 3. Schematic showing memory model parameters.

$$k_n = k_0 * D^n \quad (0 < D < 1) \qquad (6)$$

where D is a parameter of the model. The case of constant shift per stimulus, $k_n = k_0$, was also analyzed. This was a special case of *Eq. 6* where D was equal to 1.

Matching of Model to Experimental Data and Simulations

We explored ways of obtaining model parameters (a and b defining the restitution curve and k_0 and D defining the shift) from the experimental data and identified several techniques. These methods were found to be applicable for obtaining exponential restitution curve parameters as well. The results of stimulus *protocol 1* were simulated with these parameters to test the validity of the model.

RESULTS

DI,APD Pair Evolution (Stimulus Protocol 1)

When the 100 APD after BCL changes were plotted against preceding DI, three patterns in the evolution of DI and APD were seen. An example of each pattern taken from one PF experiment is shown in Fig. 4. In approximately one-half of the transitions between two BCL (34/67), all 100 (DI,APD) pairs aligned immediately on the line representing the equation DI + APD = new BCL, hereafter called the BCL line (Fig. 4*B*). In another group of transitions (30/67), the first (DI,APD) pair after the transition to new BCL lay away from the BCL line but the remaining 99 pairs aligned on the BCL line (Fig. 4*C*). Only rarely (3/67) did we see (DI,APD) pairs oscillate before aligning with the BCL line (Fig. 4*A*). In all transitions, once a (DI,APD) pair aligned with the BCL line, the remaining pairs moved up and to the left if pacing rate was slowed or down and to the right if pacing rate was increased.

Figure 5 shows the relationship between the patterns of transition and the BCL change producing them. The thickness of the lines (thinnest = 1, thickest = 6) indicate the number of transitions that showed that particular pattern. Figure 5 shows that direct alignment was likely when the BCL change was ±300 ms and between longer BCL and that alignment requiring one beat was likely when the BCL change was ±600 or 900 ms, especially when going from or going to a BCL of 400 ms. All three instances of oscillations observed were in a PF preparation. The direction of BCL change did not predispose toward either direct or one-step alignment. Other than the observation of oscillation in one PF experiment, there were no obvious tendencies for one tissue to show one pattern over another.

APD Evolution (Stimulus Protocol 1)

We also analyzed the temporal evolution of APD values independently of DI as a function of beat num-

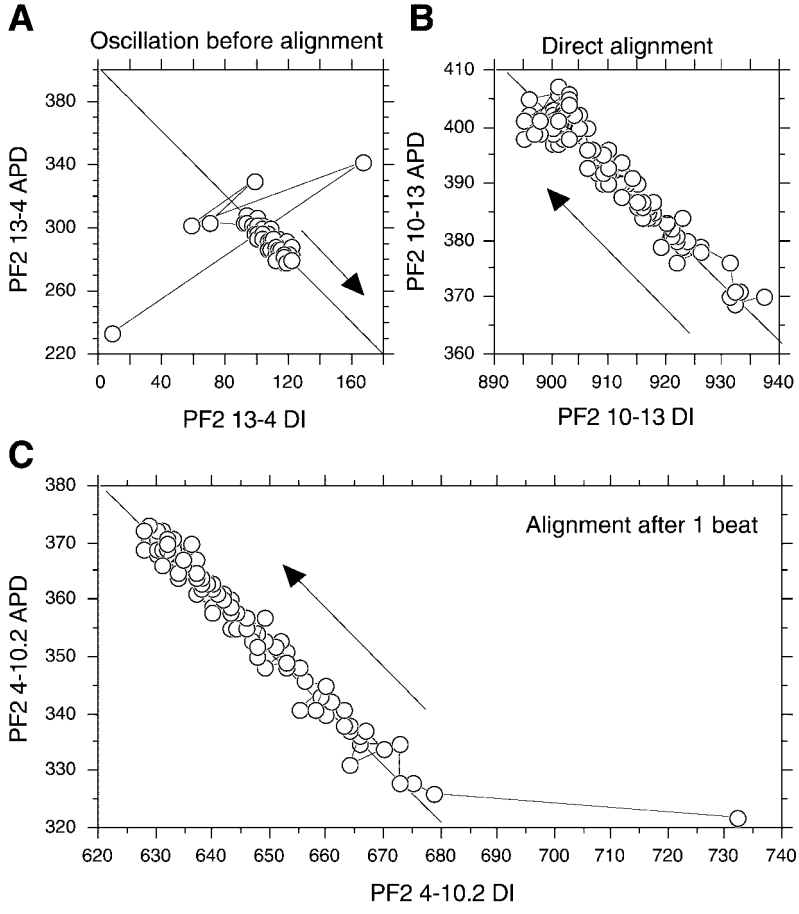

Fig. 4. The 3 different patterns of diastolic interval (DI), action potential duration (APD) pair alignment onto new BCL lines. Evolution of (DI,APD) pairs in a Purkinje fiber (PF) preparation are shown during the 100-beat transition from a BCL of 1,300 to 400 ms (*A*), 1,000 to 1,300 ms (*B*), and 400 to 1,000 ms (*C*). The diagonal line (BCL line) indicates the line where the sum of DI and APD equals the new BCL value. The 1st through 100th DI,APD pairs after the rate changes are shown. The steady-state DI,APD pair at the old BCL is not shown. (See text for further discussion.)

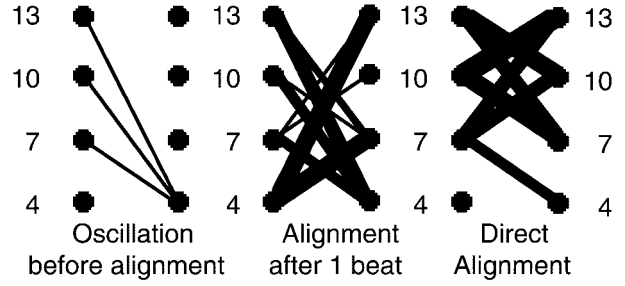

Fig. 5. Dependence of (DI,APD) transition pattern on change of BCL. BCL values of 400, 700, 1,000 and 1,300 ms are abbreviated to 4, 7, 10, and 13. The old BCL is shown on *left* and the new BCL on *right* in each panel. The lines range in thickness from 1 to 6 and indicate the number of transitions between a particular pair of BCL that showed a particular pattern. For example, the thick line connecting 4 on the left with 13 on the right in the "Alignment after 1 beat" category indicates that there were 6 transitions (all 6 tissues) from a BCL of 400 to a BCL of 1,300 that showed alignment after 1 beat. Oscillation was seen in 3 transitions, all in Purkinje, alignment after 1 beat was seen in 30 transitions (18 for a BCL increase, 12 for a BCL decrease), and direct alignment was seen in 34 transitions (14 for a BCL increase, 20 for a BCL decrease).

ber after abrupt changes in BCL using the same data as in *DI,APD Pair Evolution*. Hereafter, "APD evolution" refers to APD vs. beat number. As the example of endocardium stimulated with *protocol 1* in Fig. 6 typifies, in the majority of transitions, APD at each new BCL increased or decreased sharply at first and then less sharply. However, the slope of change rarely became zero, i.e., reached a clear plateau, within the 100 beats of our observation, even though we have drawn, by eye, approximate plateau values in Fig. 6. This slow but continuous evolution of APD is well established (17, 31). There were a few transitions where the difference between the two steady-state values were smaller than the measurement noise or where the pattern appeared to be biphasic (e.g., 1,300 → 1,000 and 700 → 1,000 in Fig. 6). Transitions showing such biphasic

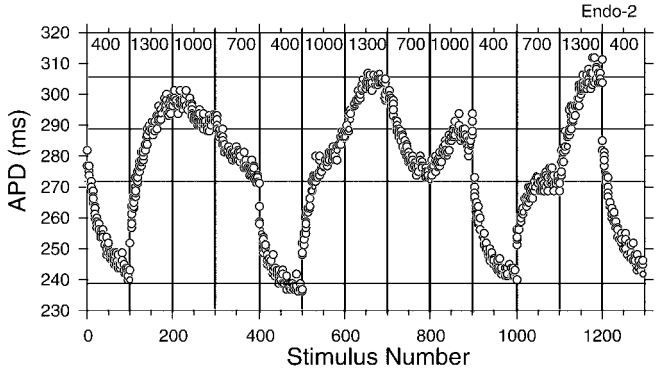

Fig. 6. APD evolution in a canine endocardial (Endo) preparation stimulated 100 times each at 4 different BCL (ms). The sequence of BCL is shown at *top*. APD did not reach an asymptotic value within the 100-stimulus train duration in the majority of transitions. Each transition was fit with a monoexponential curve for analysis (fits not shown). The 4 horizontal lines indicate approximate values that APD approached as determined by eye when pacing at the 4 different BCL.

patterns were omitted from the curve-fitting analyses described next.

Each transition segment from one BCL to another was curve fit with the exponential curve APD = $\alpha + \beta \exp(-n/\eta)$ where n is stimulus number. The different BCL combinations provided ~12 values of α, β, and η for each experiment. We studied the nine correlations between each of α, β, and η and each of old BCL, new BCL, and ΔBCL. We found in all six experiments that α was highly correlated with new BCL value (correlation coefficient range ~0.801–0.968, mean 0.883 ± 0.069; $P < 0.001$ for all) and β was highly correlated with ΔBCL (correlation coefficient range ~0.812–0.977, mean 0.925 ± 0.0631; $P < 0.0001$ for all except PF *dog 2*, in which $P = 0.006$), whereas η did not correlate with any of new BCL, old BCL, or ΔBCL ($P \geq 0.5$ for 14 of 18 fits). Each tissue gave a similar mean value of η, and the mean over the aggregate of 66 transitions was 25.91 ± 10.10. Table 1 lists the equations relating α and β to new BCL and ΔBCL values, respectively. The values in Table 1 can be used to compute expected APD evolution curve formulas for a given BCL change.

Restitution Curve Evolution (Stimulus Protocol 2)

For each tissue, 7–12 pairings of old BCL and new BCL were studied. In general, a rate increase (premature new BCL) decreased the asymptote and drop and increased the time constant, i.e., restitution curves became lower and flatter. A rate decrease (postmature

Table 1. *Formulas for computing action potential duration evolution curve parameters from pacing cycle length values*

PF *dog 2*			
α=	new BCL	×0.1302	+236
β=	ΔBCL	×0.0742	
PF *dog 3*			
α=	new BCL	×0.0475	+204
β=	ΔBCL	×0.0374	
Endo *dog 2*			
α=	new BCL	×0.0699	+215
β=	ΔBCL	×0.0565	
Endo *dog 3*			
α=	new BCL	×0.0449	+195
β=	ΔBCL	×0.0307	
Endo *dog 4*			
α=	new BCL	×0.0359	+166
β=	ΔBCL	×0.0334	
Epi *dog 1*			
α=	new BCL	×0.0239	+162
β=	ΔBCL	×0.0223	

When pacing cycle length (BCL) was changed abruptly, action potential duration (APD) increased or decreased toward a new value. These changes were fit with a function of the form: APD = $\alpha + \beta \exp(-\text{stimulus number}/\eta)$. Asymptote α was highly correlated with new BCL value, and β was highly correlated with change in BCL (ΔBCL). Linear regression produced equations relating α to new BCL and β to ΔBCL, e.g., a BCL change from 1,300 to 400 in Purkinje fiber (PF) *dog 2* would be expected to give an APD evolution curve of the formula $(400 \times 0.1302 + 236) + (900 \times 0.0742) \times \exp(-\text{stimulus number}/\eta)$. The time constant η was not affected significantly by tissue type or BCL, and the mean over 66 transitions was 25.9 ± 10.1. Endo, endocardial tissue; Epi, epicardial tissue.

new BCL) had the opposite effect, i.e., it increased the asymptote and drop and decreased the time constant. The exception to this rule was in epicardium. Drop magnitude did not show a direction of change dependent on BCL. Figure 7 shows an example of restitution curve evolution data obtained from epicardial tissue with BCL change from 1,300 to 400 ms. Fig. 7*A* corresponds to the schematic diagram in Fig. 2*A*, and Fig. 7*B* corresponds to Fig. 2*B* with results for five additional BCL transitions shown. Computation of a horizontal plus vertical restitution curve shift parameter in the curve fits did not produce fits better than those based on vertical shift alone. The change in shift parameters with increasing numbers of S2 was not necessarily monotonic, as can be seen from the restitution curve for two S2 in Fig. 7*A* and from the nonmonotonicity of the graphs in Fig. 7*B*. The following three paragraphs describe how well the data were fit by linear regression.

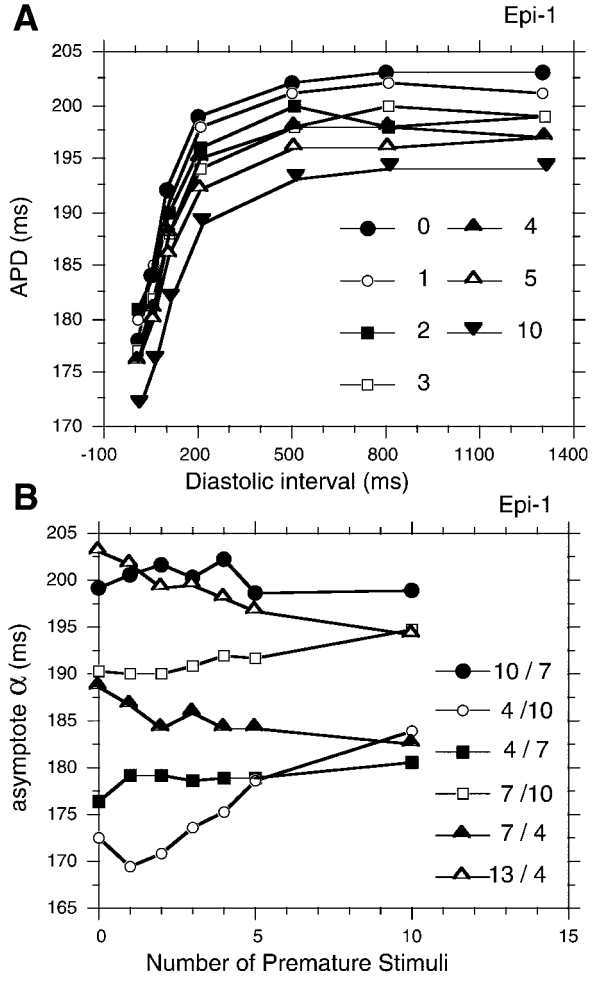

Fig. 7. Restitution function evolution due to cardiac memory. Example of restitution curve evolution data obtained from epicardial (Epi) tissue. *A*: the conventional restitution curve measured at BCL of 1,300 ms is shown at *top*. As increasing numbers of premature stimuli (1–10) with BCL of 400 ms were given, the restitution curve shifted downwards. *B*: the restitution curves in *A* were fit with monoexponential curves. The asymptotes of those curves were plotted against the number of premature stimuli (○). Plots of asymptotes are shown for other BCL changes as well. A symbol key of 4/7 indicates a BCL change from 400 to 700 ms.

In epicardium ($n = 2$; pooled data), dependence of the restitution parameters on number of stimuli at new BCL was statistically significant for 8 of 14 transitions for the asymptote, whereas drop and time constant value dependence were statistically significant for 0 and 2 of 14 transitions, respectively. However, for time constant, the direction of change was similar to the other tissues (increasing with premature new BCL, decreasing with postmature BCL) for 11 of 14 transitions. This result is interpreted to mean that the correct trend for time constant change was present but was not enough to overcome the experimental noise. The rate of change of asymptote and time constant over number of extrastimuli (i.e., slope of α and slope of τ in a Fig. 2*B*-type plot) depended on ΔBCL with $P = 0.16$ and 0.0001, respectively (i.e., the slope of these slopes in a Fig. 2*D*-type plot was different from zero with the given P values).

In endocardium ($n = 1$), dependence of the restitution parameters on number of stimuli at new BCL was statistically significant for four, six, and four of seven transitions for the asymptote, drop, and time constant values. The direction of change for the restitution parameters was similar to the other tissues (lower and flatter restitution curves with premature new BCL, higher and steeper curves with postmature new BCL), with six, six, and seven of seven transitions being consistent with the general trend for asymptote, drop, and time constant, respectively. The rate of change of asymptote, drop, and time constant over number of extrastimuli depended on new BCL with $P = 0.0007$, 0.002, and 0.0003, respectively (i.e., the slope of these slopes in a Fig. 2*C*-type plot was significantly different from zero).

In PF ($n = 2$; pooled data), dependence of the restitution parameters on number of stimuli at new BCL was statistically significant for 13, 5, and 2 of 20 transitions for the asymptote, drop, and time constant values, respectively. The small number of significant linear fits for asymptote and drop was due to the presence of oscillations of those parameters depending on whether the number of stimuli at the new BCL was even or odd. Nevertheless, if the data were fit with straight lines, the direction of change for the restitution parameters was similar to the other tissues (lower and flatter restitution curves with premature new BCL, higher and steeper curves with postmature new BCL), with 18, 17, and 17 of 20 transitions being consistent with the general trend for asymptote, drop, and time constant, respectively. The rate of change of asymptote, drop, and time constant over number of extrastimuli depended on ΔBCL with $P = 0.0001$, 0.0005, and 0.12, respectively.

Table 2 summarizes the formulas that describe how restitution curves evolve when BCL is changed from one value to another in the different ventricular tissue types. The formulas were obtained from the curve fits just described and can be used for restitution curve prediction.

Table 2. *Formulas for computing slopes and intercepts of parameters describing restitution functions from BCL values*

	Intercept	SE	Coefficient	SE	BCL Parameter
I Epi_α	158.7	±3.65	+0.03488	±0.00418	×Old BCL
S Epi_α	0		+0.00118	±0.00078	×ΔBCL
I Epi_β	31.5	±1.20			
S Epi_β					
I Epi_τ	181.6	±19.69	−0.05821	±0.02255	×Old BCL
S Epi_τ	0		−0.00525	±0.00189	×ΔBCL
I $Endo_\alpha$	165.8	±5.24	+0.03681	±0.00621	×Old BCL
S $Endo_\alpha$	0		+0.00354	±0.00048	×New BCL
I $Endo_\beta$	5.813	±3.611	+0.02626	±0.00428	×Old BCL
S $Endo_\beta$	0		+0.00316	±0.00055	×New BCL
I $Endo_\tau$	185.1	±19.74	−0.12118	±0.02338	×Old BCL
S $Endo_\tau$	0		−0.01555	±0.00325	×New BCL
I PF_α	209.1	±11.28	+0.07072	±0.01393	×Old BCL
S PF_α	0		+0.00272	±0.00045	×ΔBCL
I PF_β	73.34	±11.17	+0.02733	±0.01379	×Old BCL
S PF_β	0		+0.00163	±0.00035	×ΔBCL
I PF_τ	128.8	±27.2			
S PF_τ	0		−0.00242	±0.00108	×ΔBCL

Values were obtained from the data as illustrated in Fig. 2. *I*, intercept; *S*, slope. The standard restitution function equation (0 prematures) would be expressed as APD = $I_\alpha - I_\beta * \exp(-\mathrm{DI}/I_\tau)$. As an example, to compute the restitution curve that would be obtained after $n = 3$ premature stimuli at a cycle length of 400 after steady-state pacing at a cycle length of 1,200 in epicardium, one would use the formula: APD = [(159 + 0.035 × oldBCL) + (0.00118 × ΔBCL × n)] − [32] × exp(−DI/[(182 − 0.058 × oldBCL) + (0.005 × ΔBCL × n)] = [159 + 0.035 × 1,200 + 0.00118 × 800 × 3] − 32 exp[−DI/(182 − 0.058 × 1,200) + (0.005 × 800 × 3)] = 204 − 32 exp(−DI/124).

Dynamics of Linear Restitution Model

We analyze here the dynamics of the model described in MATERIALS AND METHODS.

Case of exponentially decreasing vertical shift. From *Eqs. 1* and *2* we obtain

$$y_{n+1} = a * (\mathrm{T} - y_n) + b - K_n \quad (7)$$

Likewise

$$y_n = a * (\mathrm{T} - y_{n-1}) + b - K_{n-1} \quad (7')$$

Subtracting *Eq. 7* from *Eq. 7′* gives us

$$y_n - y_{n+1} = -a * (y_{n-1} - y_n) + k_{n-1} \quad (8)$$

or using the definition in *Eq. 4*

$$d_n = -a * d_{n-1} + k_{n-1} \quad (9)$$

Simply to eliminate multiple parentheses, let

$$c = -a \quad (10)$$

Iterating and expanding *Eq. 9* gives

$$d_n = c^n * d_0 + k_0 * (c^n - D^n)/(c - D) \quad (11)$$

or

$$d_n = c^n * [d_0 + k_0/(c - D)] - D^n * [k_0/(c - D)] \quad (11')$$

In the limit of n increasing to infinity, if both

$$|c| = |a| < 1 \quad (12a)$$

and

$$D < 1 \quad (12b)$$

then d_n converges to 0

$$\lim_{n \to \infty} d_n = 0 \quad (13)$$

The physiological interpretation of *Eq. 13* is that slope of the APD evolution curve (not of restitution) gradually decreases to zero and APD achieves a steady-state value after a BCL change. *Equation 11′* shows that for large n, d_n diminishes as the nth power of the larger of D and c. When n is small, oscillatory APD behavior is possible because $c < 0$, and c^n changes sign depending on whether n is odd or even. The amplitude of the DI,APD oscillations are determined by $d_0 + k_0/(c - D)$. Large-amplitude oscillations would be expected when this term is large because of a large change of BCL (large d_0), restitution slope (large d_0), or vertical shift of restitution (large k_0). The attenuation of oscillations is dependent on c, with a time constant equal to the reciprocal of $\ln c$, i.e., large c would produce longer duration oscillations, whereas c close to 0 would produce immediate attenuation of the oscillations.

Case of constant k. When $D = 1$, $k_n = k_0$ for all n and

$$d_n = c^n * d_0 + k_0 * (1 - c^n)/(1 - c) \quad (14)$$

and for convergence criterion (*Eq. 12a*)

$$\lim_{n \to \infty} d_n = -k/(1 + a) \quad (15)$$

The physiological interpretation of *Eq. 14* is that oscillations of APD will increase in amplitude (which in real tissue would eventually result in a stimulus failing to excite the tissue because of long refractory period) if the slope of the linear restitution curve is >1, dampen if the slope is >1, and stay at a fixed amplitude if the slope is exactly 1. The physiological interpretation of *Eq. 15* is that for large n, APD continues to decrease or increase forever after a BCL change, by the fixed amount $-k/(1 + a)$. This means that the slopes of the APD evolution curves should never become zero but asymptotically approach the constant value $-k/(1 + a)$ after the initial oscillatory phase has passed. Therefore, the constant k case is a good model for the behavior of the APD evolution curves in which APD continues to decrease or increase indefinitely, i.e., fails to reach a plateau, as observed in some BCL changes (Fig. 6). We also note that in the constant k case, the transients of d_n diminish at a rate of c^n $[d_0 + k/(1 - c)]$.

Case of horizontal + vertical shift. The case of horizontal shift is easily extrapolated from the vertical shift case in the linear restitution model. A downward shift of k coupled with a leftward shift of λ is equivalent to a downward shift of $k - a * \lambda$ and *Eq. 11* becomes

$$d_n = c^n * d_0 + k_0 * (c^n - D^n)/(c - D) + \lambda_0 * (c^n - L^n)/(c - L) \quad (16)$$

where leftward shift λ_n is described by exponentially decreasing function $\lambda_0 * L^n$ where L is a model parameter.

Obtaining Model Parameters from Experimental Data

Ideally, one would like to obtain parameters for the dynamic model quickly without having to apply time-consuming stimulus protocols to every new patient or tissue specimen. The two categories of parameters that need to be found are those that describe the restitution function and those that describe the vertical shift.

Finding parameters for linear restitution model. In the linear restitution model, there are four parameters, a and b, which describe the linear restitution curve, and k_0 and D, which describe the vertical shift of the restitution curve. In theory, one could use any four random data points from the APD evolution data to solve four equations with four unknown values. For example, for the constant k case, where $D = 1$, $y_1 = ax_1 + b$, $y_2 = ax_2 + b - k$, and $y_3 = ax_3 + b - 2k$ can be solved to give $a = (y_1 + y_3 - 2y_2)/(x_1 + x_3 - 2x_2)$, $b = y_1 - ax_1$, and $k = (y_1 - ax_1) - (y_2 - ax_2)$. In practice, however, unless the data cover a wide range of x or y values, for example, by oscillating, the differences between x or y values are small and comparable to the order of experimental noise. This makes accurate calculations of the parameters using randomly selected data points impossible. Instead, we use the fact that (x_0,y_0), the steady-state DI,APD values at old BCL, and (x_1,y_1), the DI,APD values associated with the first stimulus at the new BCL, lie on the same restitution curve $f(x)$ (see Fig. 3). This gives us values for a and b.

$$a = (y_0 - y_1)/\Delta\text{BCL} \quad (17)$$

$$b = y_0 - a * (\text{old BCL} - y_0) \quad (18)$$

k_0 is the difference between the standard restitution curve and the restitution curve after one extrastimulus. Therefore

$$k_0 = y_2 - f(x_2) \quad (19)$$

$$= y_2 - [a + b * (\text{new BCL} - y_1)] \quad (20)$$

Finally

$$y_0 - y_n = \sum_{i=0}^{n} d_i \quad (21)$$

which for large n

$$= d_0/(1 - c) + k_0/[(1 - c)(1 - D)] \quad (22)$$

under convergence criteria (*Eqs. 12a* and *12b*). Solving this for D gives

$$D = 1 - k_0/[(y_0 - y_n)(1 - c) - d_0] \quad (23)$$

In summary, a, b, k_0, and D can be obtained from the first three and last values of APD evolution data y_0, y_1, y_2, and y_n, where n is large enough for APD to have reached a plateau value.

If y_n does not reach a plateau value, we assume a constant k case. With *Eq. 15*, k can be computed as

$$k = -\text{evolution curve slope} * (1 + a) \quad (24)$$

Finding parameters for exponential restitution model. Two of the three parameters for a monoexponential restitution curve can be obtained similarly to *Eqs. 17* and *18* from the first two values of APD evolution data. For example

$$\beta = (y_0 - y_1)/[\exp(-x_0/\tau) - \exp(-x_1/\tau)] \quad (25)$$

$$\alpha = y_0 - b * \exp(-x_0/\tau) \quad (26)$$

It is necessary to obtain the third parameter, in this example τ, either from a table of normal values or by using an S1S2 protocol to obtain one more DI,APD value to establish the restitution function.

The parameter k_0 is obtained as in *Eq. 19*

$$k_0 = [\alpha + \beta * \exp(-x_2/\tau)] - y_2 \quad (27)$$

To obtain D, we use

$$y_n = \alpha + \beta * \exp(-x_n/\tau) - (k_0 + k_1 + \cdots + k_{n-2}) \quad (n > 2) \quad (28)$$

and

$$(k_0 + k_1 + \cdots + k_{n-2}) = k_0/(1 - D) \quad (29)$$

for very large n. The last two equations solved for D give

$$D = 1 - k_0/[\alpha + \beta * \exp(-x_n/\tau) - y_n] \quad (30)$$

When n is large, y values are not changing much, so x_n can be substituted by new BCL $- y_n$. In summary, two of the three parameters defining the exponential restitution curve and the two parameters defining the shift of restitution with each stimulus can be obtained from the first three and last values of APD evolution data y_0, y_1, y_2, and y_n, where n is large enough for APD to have reached a plateau value.

Special case of restitution curve reconstruction from oscillatory data. We discovered a crude visual method by which a nonlinear restitution curve and early shift values could be reconstructed simultaneously in the special case where DI,APD pairs oscillate several times, thereby providing a wide range of DI points. In this method, (DI_1, APD_1), $(DI_2, APD_2 - k)$, $(DI_3, APD_3 - 2k)$, . . ., $[DI_n, APD_n - (n - 1) * k]$ are plotted for the n oscillating (DI,APD) pairs for various values of k until the curve produced by connecting the points resembles an exponential restitution curve. For example, the first five DI,APD pairs measured from the BCL 1,300 to 400 ms data of a PF experiment (Fig. 4*A*) were found to produce the smoothest restitution curve when the five pairs were plotted with a k value of 5 ms. The restitution curve found for this data set using this method was

$$\text{APD} = 352 - 148.6 * \exp(-\text{DI}/42) \quad (31)$$

Cross-Validation of Model by DI,APD Evolution Simulation

We reconstructed restitution curve evolution for the 60 experimental runs of stimulus *protocol 1* with *Eqs. 25–30* and τ from Table 2. We found that in practice,

β was unrealistically large if the difference between y_0 and y_1 was small (≤5). This was true of 25 of 60 runs. Furthermore, if the difference between y_1 and y_2 was small, the k_0 value was unrealistically small or of the wrong sign. This was true of a further nine runs. Reconstructions of DI,APD pair evolution for the remaining 26 runs produced results quantitatively and qualitatively similar to the original experiments, especially for the cases in which the behavior was simple with immediate or almost immediate alignment of DI,APD pairs on the BCL line. We show in Fig. 8*A* the results of simulation of the most complex behavior, i.e., the oscillatory DI,APD evolution of the PF going from BCL of 1,300 to 400 ms shown in Fig. 2*A*. The main difference between the simulation and the original data was in the position of the third, fourth, and fifth points relative to the first and second points. In the experiment, the APDs of those points are higher.

We hypothesized that the conclusions drawn from the analysis of the linear restitution model (*Eq. 11*) would hold to a first approximation for the exponential restitution case, i.e., that a greater change of BCL and steeper restitution slope (greater β and smaller τ) would lead to a larger amplitude of oscillation and that a steeper restitution slope would lead to a longer duration of oscillation. This is shown to be true in Fig. 8, *B* and *C*, in which a small and large restitution slope are compared. A comparison of Fig. 8*A* vs. 8*B* and 8*C* also shows that a small k_0 is responsible for a lower position of the first and second APD values relative to the subsequent values.

DISCUSSION

History of Research in Cardiac Memory and Restitution

APD is known to be a function both of immediately preceding DI or coupling interval and of previous activation history (12, 13). In general, APD of a premature activation is shorter when the DI or coupling interval is shorter (30), a dependence that has come to be called electrical restitution (1) after its similarity to mechanical restitution (4). APD is also dependent on heart rate, usually being longer at slow heart rates (20, 33, 47) as seen in prolongation of QT intervals at slow heart rates on the surface electrocardiogram. This dependence of APD and refractory period on activation history (32) is also manifest in the downward shift of the restitution curve at fast heart rates (2, 5) and has come to be called cardiac memory (22, 8) because the tissue tends to have longer APD than expected from DI if previous APD were long, and vice versa, as though remembering its previous APD. The function of memory is to optimize the ratio of diastolic filling time to systolic ejection time.

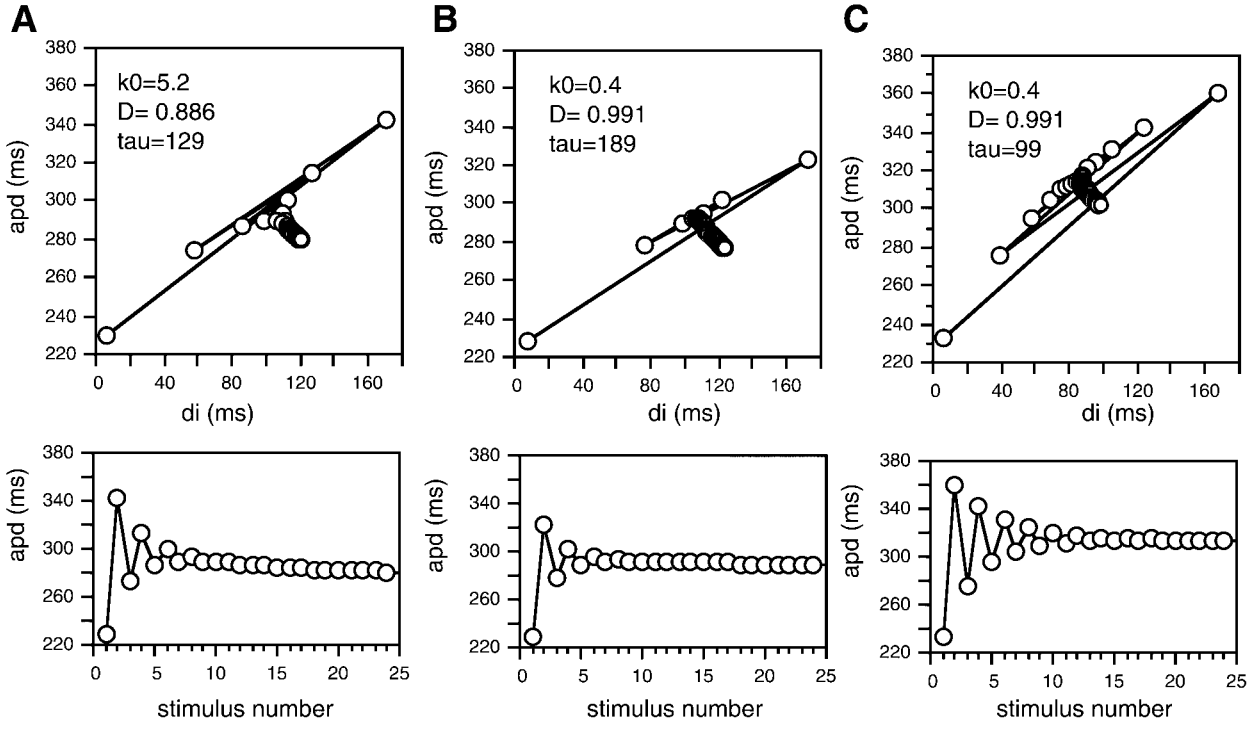

Fig. 8. Cross-validation of mathematical model by simulation of DI,APD evolution. *Top panels*: DI,APD evolution in the DI,APD plane. *Bottom panels*: APD evolution as a function of beat number. *A*: the oscillatory DI, APD evolution of the Purkinje fiber shown in Fig. 2*A* was simulated using model parameters extracted from the data as described in the text. The parameters were old BC = 1,300, new BCL = 400, α = 393, β = 172, τ = 129, k_0 = 5.2, and D = 0.89. *B*: a smaller restitution slope dampened oscillation amplitude and duration. *C*: a greater restitution slope increased oscillation amplitude and duration.

Suggestion for New Memory Terminology

The shift of restitution curve with change to new cycle lengths is an effect of memory. When switching to a new pacing rate, the restitution curve does not jump immediately to the new restitution curve but is somewhere between the old and the new. Therefore, one might say that the curve still remembers and lingers near the old curve. In that sense, more memory implies smaller or slower shifts to the new state. This is the sense used when stating that ventricular muscle has more memory than Purkinje tissue, because a premature stimulus changes the refractory period less in ventricular muscle than in the Purkinje system (28). In other words, more memory means less memory effect, and this is confusing. We therefore suggest use of another term, accommodation (27), as an inverse concept of memory. It is short compared with other terms used historically, such as cumulative effect (17), information retention (14), and cycle length-independent change (12). Greater restitution curve shifts and greater dynamic restitution curve slope could be attributed to greater accommodation. This term would abolish the need for circumlocutions such as "declining memory effect" to describe the shift of restitution curves after rate changes. It would also be useful in differentiating short-term memory, such as we analyzed in this study, from changes in T wave polarity induced by ventricular pacing that persist for hours to weeks after resumption of normal atrioventricular conduction, a phenomenon that is also referred to as cardiac memory (6, 40, 41).

Methods of Cardiac Memory/Accommodation Quantification

The standard restitution curve is always sufficient for explaining changes in APD after one premature stimulus, because restitution is defined and measured as the relationship between one premature stimulus coupling interval or DI and the following APD at a particular pacing rate. It is measured directly, and no assumptions are made. However, when there is more than one premature stimulus, APD values deviate more and more from that predicted from the restitution curve because of the effects of accommodation. There is no universally accepted way of quantifying accommodation. One can normalize steady-state restitution curves (5, 8) and regard the normalization factor as a measure of memory. This normalization factor has been used to model the memory effect and its role in spiral wave breakup (10), although normalization with the steady-state restitution curves is predicated on making assumptions about the time course of restitution change between two steady states. Two theoretical models of memory have treated it as a variable that gets incremented with every action potential but also decays with time (16, 34), i.e., memory increases when there are many action potentials per unit time and decreases with long DI. The latter model successfully reproduces qualitative aspects of complex alternans phenomena seen in experiments that cannot be simulated by iteration of a standard restitution curve. The model presented in this study does not attempt to characterize accommodation by an independent variable as in the two theoretical studies. It is a simple phenomenological model in which accommodation is characterized by the initial restitution curve shift value and its decay with additional extrastimuli.

Experimental Results

The results of the *protocol 1* demonstrated two things. First, as shown by other investigators (17, 31), APD frequently does not equilibrate to a new steady-state value within 100 beats of a change to new BCL. Instead, the APD continues changing beyond 100 beats, or if the change is between two relatively long BCL APD can increase then decrease, or decrease then increase. This means that it is sometimes difficult to define steady-state APD, or for that matter, restitution function, for a given BCL. Second, oscillation of DI,APD pairs in the DI,APD space before alignment on the DI + APD = new BCL line was rare. This was to be expected. For example, Saito et al. (42) noted that the maximum BCL producing oscillations in canine ventricular tissue was <400 ms, whereas the minimum BCL used in this study was 400 ms. Oscillation in the present study was seen only in PF when the new BCL was very short. The mathematical model provided three conditions for oscillation of DI,APD evolution to occur, all of which were satisfied in the PF that showed oscillation. In the three oscillations that did occur, the pattern of DI,APD pairs oscillating back and forth on a single line for many beats, followed by alignment on the BCL line as described by Vick (48), was not observed. In simulations such as Fig. 8*A*, however, we were able to reproduce similar behavior, which leads us to believe that such patterns can occur experimentally.

The results of the *protocol 2* showed that the parameters of the monoexponential curve fits to restitution could be treated as changing linearly with increasing numbers of premature stimuli up to 10 stimuli. As might be expected, the changes were proportional to difference between new and old BCL. In general, faster pacing flattened and lowered restitution curves whereas slower pacing sharpened and raised restitution curves, as seen in cat papillary muscle (2) and canine PF (8). Epicardium was an exception in that drop magnitude did not show a direction of change related to BCL. It was also found that computation of a horizontal + vertical restitution curve shift parameter in the curve fits produced fits no better than those based on vertical shift alone.

Earlier studies studying the shift of restitution curves produced by multiple S2 using finer DI spacing showed that the slope of the early part (short DI) of the restitution curve was sharper for the second S2 (restitution curve after 1 premature stimulus) than for the first S2 (the standard restitution curve) (24, 51). A reappraisal of the plots of the drop parameter against number of premature stimuli confirms the earlier re-

sults in that the drop parameter is frequently larger for the second S2 in endocardium and Purkinje (not shown), usually in the transition from a large BCL to a BCL of 400 ms. However, the results of the present study (transient increase of slope followed by flattening of restitution curve slope over 10 premature S2) do contradict the earlier results seen in Purkinje (increased slope maintained over 4 premature S2; Ref. 51). This may be due to the larger number of prematures applied in the current study or to the difference between refractory period and APD restitution, but it is most likely due to the fact that new BCL was set at the minimum in the earlier study (effective refractory period of the last S1 beat + 10 ms). This interpretation is more likely because of the known steeper slope of dynamic restitution at shorter BCL (25), although dynamic and standard restitution cannot be compared directly.

We never saw biphasic APD restitution curves (11, 21, 24, 50) in which the ventricular myocardial restitution curve has a local maximum at short DI. The action potentials at this peak have been referred to as supernormal premature action potentials (3) and are believed to reflect potentiation of the calcium current. The prevalence of biphasic restitution curves as opposed to monotonically increasing restitution curves is not known. The probable reason we did not see obvious APD peaks, assuming some had been present, was the coarse resolution measurements of restitution curves.

Modeling Results and Implications

Mathematical analysis of the dynamics where restitution curves were modeled as linear functions provided the conditions under which DI,APD oscillations would be expected after a rate change. Two factors determine whether oscillations are detectable or not, amplitude and duration of oscillation. Both the amplitude and duration have to be large for oscillation to be visible. For example, if amplitude were large but attenuation occurs in one beat, no oscillation would be seen. Oscillation is also missed if attenuation occurs slowly but amplitude of oscillation is smaller than the experimental noise. Therefore, oscillation is predicted to be visible when the restitution curve slope is steep, the BCL change is large, and vertical shift is large. Of these three criteria, the first is well known mathematically to produce APD alternans. The other two criteria are presented here for the first time.

Lepeschkin (29) hypothesized that electrocardiographic alternans at fast heart rates was due to APD dependence on preceding DI, coupled with DI alternans during alternans. Subsequently, some investigators confirmed this hypothesis whereas others found otherwise (7, 45). It was later argued that the conflicting experimental results arose from the fact that Lepeschkin's theory was applicable to Purkinje tissue but not to ventricular myocardium in that intracellular calcium concentration was also a factor contributing to APD (46). For example, Saito et al. (42) compared electrical alternans produced in both tissues. In their study, memory was accounted for by plotting the difference between two sequential APD values (Δy) against the difference between APD values obtained by projection of sequential DI values onto the restitution curves (Δy^{rtt}), i.e., the difference between APD in the absence of a memory effect. In PF, they found $\Delta y = 1.02\Delta y^{rtt} - 1.6$, whereas in myocardium, $\Delta y \approx 2\Delta y^{rtt}$, i.e., PF data gave a slope of 1 and myocardium a slope of 2. In terms of the linear restitution model developed here, $\Delta y^{rtt} = c * d_{n-1}$. From *Eq. 11* we obtain

$$\Delta y^{rtt} = d_n - k_0 * D^{n-1} = \Delta y - k_0 * D^{n-1} \qquad (32)$$

This means that a plot of Δy vs. Δy^{rtt} should give $\Delta y = \Delta y^{rtt} + \mu$, where μ is some positive value. That is, the model predicts a slope of 1. If $k_0 * D^{n-1}$ is close to 0 [$n < 4$ in Saito et al. (42)] then the model result matches the results of Saito et al. in PF and APD values during alternans are indeed a result of restitution plus effects of accommodation. What then does one make of the slope = 2 results in myocardium? Is our model of accommodation inapplicable to myocardium? Figure 7 in the report by Saito et al. (42) gives a clue. The initial shift k_0 appears to be large in ventricular myocardium compared with later shifts, judging from the large space between the restitution curve and later points. Because d_1 is greater than d_1^{rtt} by k_0 and d_2 is greater than d_2^{rtt} by $k_0 * D$, if both d_1^{rtt} and d_2^{rtt} are positive, one can easily get a slope of Δy vs. $\Delta y^{rtt} > 1$. In other words, if the term $k_0 * D^{n-1}$ is comparable to or greater than Δy^{rtt}, then one can indeed get a slope of 2 or even higher. Furthermore, Δy^{rtt} is seen to be small compared with the PF case, making it more likely for the term $k_0 * D^{n-1}$ to outweigh the Δy^{rtt} term. In other words, our model shows that it is still possible to explain ventricular myocardial APD by using the concepts of restitution and accommodation as in PF and that the particular argument used by Saito et al. cannot be used to diminish the role of electrical restitution and memory in determining APD in myocardial tissue. That said, the model does not negate the importance of intracellular calcium concentration in determination of myocardial APD. Changes to intracellular calcium concentration affect APD restitution (24) and APD alternans (19, 26, 43). We conjecture that the calcium concentration determines APD restitution and accommodation and that the two can be measured and modeled decoupled from calcium concentration without consequence because they already encode the calcium concentration information.

A study by Hirata et al. (18) reviewed some experimental literature and made the point that APD alternans could be of two types, even or odd. The odd type refers to alternans where the odd numbered beats (beat 1 being the first APD at the shortened cycle length) have the longer APD. They noted that the odd type was seen more commonly in myocardium than in Purkinje and that the even type was usually seen with a large change in BCL. If there were no accommodation at all, one would expect to see only even-type alternans. A shift in the phase can be hypothesized to occur in two ways: one is the presence of a biphasic restitu-

tion curve, and the other is to take into account the accommodation effect. From *Eq. 9*, $d_1 = -a * d_0 + k_0$ is true. The sign of d_0 is always positive for a shortening of BCL. However, the sign of d_1 can be either positive or negative depending on the relative sizes of the various parameters. If d_1 is negative, even-type alternans follows. The sharper slope a of PF restitution is in agreement with this expected result. This equation also explains why even-type alternans is more likely with a larger change of BCL; d_0 is larger in that case. If restitution slope a is smaller as in ventricular myocardium and k_0 is large, d_1 can be positive, thereby shifting the phase from even to odd-type alternans.

Cross-Validation of Model

Finding model parameters from the experimental data was not as simple as expected from theory. This was due mainly to the relatively large size of experimental noise compared with the small changes of APD during APD evolution. Nevertheless, we proposed several methods for obtaining model parameters requiring the measurement of only the first few DI,APD values and the 100th DI,APD value after a rate change. These parameters could be applied toward construction of either a linear or exponential restitution curve model. Simulation of the simple behavior (immediate or almost immediate alignment) produced realistic results. Simulation of the most complex behavior, oscillatory DI,APD in PF, was similar to experiment quantitatively and qualitatively except in one respect. This was in the positions of the early data pairs relative to the first two data pairs. The most likely cause of this discrepancy was the assumption of linear change in asymptote and drop parameters with increasing stimulus number. In the current experiments, the asymptote and drop parameters of the restitution curves showed small oscillations in PF after BCL change to very rapid rates, but this behavior was not captured in the linear regression analyses of the parameters over stimulus number. We had measured restitution curves after 0–5 and 10 S2 stimuli, which meant that there were only seven data points per parameter that could be fitted by regression analysis. This was enough for linear regression but not enough for exponential curve fitting.

Limitations

Our model assumed that the restitution curve was linear and that the slope of that curve was fixed, although the results of stimulus *protocol 2* showed that drop and time constant also evolved. These assumptions were justified by the fact that, in the absence of oscillations, only a small part of the restitution curve was explored by the dynamics of the tissues. However, at shorter BCL, where alternans is obligatory, these assumptions will no longer hold. It did appear, nevertheless, that conclusions drawn from the linear restitution model about the conditions producing longer or larger alternans were applicable to simulations using exponential restitution curves.

We reduced the dynamics of shift parameter k to two cases, that of a constant k and that of an exponentially decreasing k, and limited our analyses to those cases. However, accommodation very likely involves several mechanisms at the cellular level, each with a different time scale. Therefore, models with more complicated dynamics of k, such as where k is a sum of a constant and exponentially decreasing function, or where there are two or more time constants to the decrease of k may provide a better fit to experimental data, especially if it is of such duration that it spans the multiple time scales.

We deliberately selected our minimum BCL of pacing to be 400 ms to avoid alternation of steady-state APD. If we had selected a shorter minimum BCL with the likelihood of alternating steady-state APD value, two restitution curves would have had to be measured for a given BCL (35, 38). Consequently, experimental design prevented us from seeing oscillatory DI,APD behavior. Future experiments will focus on analysis of accommodation at short BCL, now that a framework for analyzing accommodation at longer BCL has been established.

We did not use a large number of animals for this study for several reasons. Canine restitution data is ubiquitous in the literature, especially at the relatively long BCL that we presented here. Our goal was to collect enough data to validate our mathematical model of accommodation and thus present a new way of quantifying and analyzing restitution data. The ultimate utility of the model is expected to be in its application to the computation of dynamic restitution at short BCL, to assess the role of accommodation at the short cycle lengths present in ventricular tachycardia and fibrillation.

Summary

We began with the concept that memory is the amount by which restitution curves are shifted with pacing rate change. We measured these shifts experimentally in ventricular endocardium, epicardium, and PF tissues and constructed a simple phenomenological model of memory amenable to rigorous mathematical analysis. We assessed ways of obtaining model parameters from minimum subsets of the data and finally tested the model predictions against the data. The close match of the simulations to the data suggest that memory/accommodation for a particular cycle length change can be modeled to a first approximation as a vertical shift of restitution curve. The model also produced clear predictions about the dynamic behavior of APD after an abrupt cycle length change that was able to explain several phenomena seen in the literature.

The authors thank Dr. Robert F. Gilmour, Jr. at Cornell University for the extensive use of his laboratory and for encouragement and support and Mark L. Riccio for critical assistance with data collection and transfer.

M. A. Watanabe was supported by National Heart, Lung, and Blood Institute National Research Service Award F32-HL-10308-01 and by the Cardiology Department of the Royal Infirmary of Glas-

gow. M. L. Koller was supported by a research fellowship grant from the Deutsche Forschungsgemeinschaft (Ko 1782/1-1).

REFERENCES

1. **Bass BG.** Restitution of the action potential in cat papillary muscle. *Am J Physiol* 228: 1717–1724, 1975.
2. **Boyett MR and Jewell BR.** A study of the factors responsible for rate-dependent shortening of the action potential in mammalian ventricular muscle. *J Physiol (Lond)* 285: 359–380, 1978.
3. **Boyett MR and Jewell BR.** Analysis of the effects of change in rate and rhythm upon the electrical activity in the heart. *Prog Biophys Mol Biol* 36: 1–52, 1980.
4. **Braveny P and Kruta V.** Dissociation de deux facteurs: restitution et potentiation dans l'action de l'intervalle sur l'amplitude de la contraction du myocarde. *Arch Int Physiol Biochim Biophys* 66: 633–652, 1958.
5. **Colatsky TJ and Hogan PM.** Effects of external calcium, calcium channel-blocking agents, and stimulation frequency on cycle length-dependent changes in canine cardiac action potential duration. *Circ Res* 46: 543–552, 1980.
6. **Costard-Jäckle Goetsch B, Antz M, and Franz MR.** Slow and long-lasting modulation of myocardial repolarization produced by ectopic activation in isolated rabbit hearts. Evidence for cardiac memory. *Circulation* 80: 1412–1420, 1989.
7. **Edmands RE, Greenspan K, and Fisch C.** Effect of cycle-length alteration upon the configuration of the canine ventricular action potential. *Circ Res* 19: 602–610, 1966.
8. **Elharrar V and Surawicz B.** Cycle length effect on restitution of action potential duration in dog cardiac fibers. *Am J Physiol Heart Circ Physiol* 244: H782–H792, 1983.
9. **Endresen K, Amlie JP, Forfang K, Simonsen S, and Jensen O.** Monophasic action potentials in patients with coronary artery disease: reproducibility and electrical restitution and conduction at different stimulation rates. *Cardiovasc Res* 21: 696–702, 1987.
10. **Fenton FH, Evans SJ, and Hastings HM.** Memory in an excitable medium: a mechanism for spiral wave breakup in the low-excitability limit. *Phys Rev Lett* 83: 3964–3967, 1999.
11. **Franz MR, Schaefer J, Schottler M, Seed WA, and Noble MIM.** Electrical and mechanical restitution of the human heart at different rates of stimulation. *Circ Res* 53: 815–822, 1983.
12. **Gettes LS, Morehouse GN, and Surawicz B.** Effect of premature depolarization on the duration of action potentials in Purkinje and ventricular fibers of the moderator band of the pig heart. Role of proximity and the duration of the preceding action potential. *Circ Res* 30: 55–66, 1972.
13. **Gibbs CL and Johnson EA.** Effect of changes in frequency of stimulation upon rabbit ventricular action potential. *Circ Res* 9: 165–170, 1961.
14. **Gibbs CL, Johnson EA, and Tille J.** An example of information retention in rabbit ventricular muscle fibres. *Biophys J* 4: 329–333, 1964.
15. **Gilmour RF Jr, Otani NF, and Watanabe MA.** Memory and complex dynamics in canine cardiac Purkinje fibers. *Am J Physiol Heart Circ Physiol* 272: H1826–H1832, 1997.
16. **Gulrajani RM.** Computer simulation of action potential duration changes in cardiac tissue. *IEEE Comput Cardiol* 244: 629–632, 1987.
17. **Han J and Moe GK.** Cumulative effects of cycle length on refractory periods of cardiac tissues. *Am J Physiol* 217: 106–109, 1969.
18. **Hirata Y, Kodama I, Iwamura N, Shimizu T, Toyama J, and Yamada K.** Effects of verapamil on canine Purkinje fibres and ventricular muscle fibres with particular reference to the alternation of action potential duration after a sudden increase in driving rate. *Cardiovasc Res* 13: 1–8, 1979.
19. **Hirayama Y, Saitoh H, Atarashi H, and Hayakawa H.** Electrical and mechanical alternans in canine myocardium in vivo. *Circulation* 88: 2894–2902, 1993.
20. **Hoffman BF and Suckling EE.** Effect of heart rate on cardiac membrane potentials and the unipolar electrogram. *Am J Physiol* 179: 123–130, 1954.
21. **Iinuma H and Kato K.** Mechanism of augmented response in canine ventricular muscle. *Circ Res* 44: 624–629, 1979.
22. **Janse MJ.** *The Effect of Changes in Heart Rate on the Refractory Period of the Heart*. Amsterdam: University of Amsterdam Mondeel Offset Drukkerij, 1971, p. 16.
23. **Karma A.** Electrical alternans and spiral wave breakup in cardiac tissue. *Chaos* 4: 461–472, 1994.
24. **Kobayashi Y, Peters W, Khan SS, Mandel WJ, and Karaguezian H.** Cellular mechanisms of differential action potential duration restitution in canine ventricular muscle cells during single versus double premature stimuli. *Circulation* 86: 955–967, 1992.
25. **Koller ML, Riccio ML, and Gilmour RF Jr.** Dynamic restitution of action potential duration during electrical alternans and ventricular fibrillation. *Am J Physiol Heart Circ Physiol* 275: H1635–H1642, 1998.
26. **Lab MJ and Lee JA.** Changes in intracellular calcium during mechanical alternans in isolated ferret ventricular muscle. *Circ Res* 66: 585–595, 1990.
27. **Lehmann MH, Denker S, Mahmud R, and Akhtar M.** Functional His Purkinje system behavior during sudden ventricular rate acceleration in man. *Circulation* 68: 767–775, 1983.
28. **Lehmann MH, Denker S, Mahmud R, and Akhtar M.** Post-extrasystolic alterations in refractoriness of the His-Purkinje system and ventricular myocardium in man. *Circulation* 69: 1096–1102, 1984.
29. **Lepeschkin E.** Electrocardiographic observations on the mechanism of electrical alternans of the heart. *Cardiologia* 16: 278–287, 1950.
30. **Mendez C, Gruhzit CC, and Moe GK.** Influence of cycle length upon refractory period of auricles, ventricles, and A-V node in the dog. *Am J Physiol* 184: 287–295, 1956.
31. **Miller JP, Wallace AW, and Feezor MD.** A quantitative comparison of the relation between the shape of the action potential and the pattern of stimulation in canine ventricular muscle and ventricular fibers. *J Mol Cell Cardiol* 2: 3–19, 1971.
32. **Mines GR.** On dynamic equilibrium in the heart. *J Physiol (Lond)* 46: 349–383, 1913.
33. **Moore EN, Preston JB, and Moe GK.** Durations of transmembrane action potentials and functional refractory periods of canine false tendon and ventricular myocardium: comparisons in single fibers. *Circ Res* 17: 259–273, 1965.
34. **Otani NF and Gilmour RF Jr.** Memory models for the electrical properties of local cardiac systems. *J Theor Biol* 187: 409–36, 1997.
35. **Pastore JM and Rosenbaum DS.** Spatial and temporal heterogeneities of cellular restitution are responsible for arrhythmogenic discordant alternans (Abstract). *Circulation* 100: I-51, 1999.
36. **Qu Z, Weiss JN, and Garfinkel A.** Spatiotemporal chaos in a simulated ring of cardiac cells. *Phys Rev Lett* 78: 1387–1390, 1997.
37. **Qu Z, Weiss JN, and Garfinkel A.** Cardiac electrical restitution properties and stability of reentrant spiral waves: a simulation study. *Am J Physiol Heart Circ Physiol* 276: H269–H283, 1999.
38. **Rhee EK, Hourigan AM, and Frame LH.** Dynamics of action potential alternans (Abstract). *Circulation* 86: I-299, 1992.
39. **Riccio ML, Koller ML, and Gilmour RF Jr.** Electrical restitution and spatiotemporal organization during ventricular fibrillation. *Circ Res* 84: 955–963, 1999.
40. **Rosen MR, Cohen IS, Danilo P Jr, and Steinberg SF.** The heart remembers. *Cardiovasc Res* 40: 469–482, 1998.
41. **Rosenbaum MB, Blanco HH, Elizari MV, Lazzari JO, and Davidenko JM.** Electrotonic modulation of the T wave and cardiac memory. *Am J Cardiol* 50: 213–222, 1982.
42. **Saito H, Bailey JC, and Surawicz B.** Alternans of action potential duration after abrupt shortening of cycle length: differences between dog Purkinje and ventricular muscle fibers. *Circ Res* 62: 1027–1040, 1988.
43. **Saito H, Bailey JC, and Surawicz B.** Action potential duration alternans in dog Purkinje and ventricular muscle fibers. Further evidence in support of two different mechanisms. *Circulation* 80: 1421–1431, 1989.
44. **Samie FH, Mandapati R, Gray RA, Watanabe Y, Zuur C, Beaumont J, and Jalife J.** A mechanism of transition from ventricular

fibrillation to tachycardia. Effect of calcium channel blockade on the dynamics of rotating waves. *Circ Res* 86: 684–691, 2000.
45. **Spear JF and Moore EN.** A comparison of alternation in myocardial action potentials and contractility. *Am J Physiol* 220: 1708–1716, 1971.
46. **Surawicz B and Fisch C.** Cardiac alternans: diverse mechanisms and clinical manifestations. *J Am Coll Cardiol* 20: 483–499, 1992.
47. **Trautwein W and Zink K.** Über Membran und Aktionspotentiale einzelner Myokardfasen des Kalt und Warmblüterherzens. *Arch Ges Physiol* 256: 68–84, 1952.
48. **Vick RL.** Action potential duration in canine Purkinje tissue: effects of preceding excitation. *J Electrocardiol* 4: 105–115, 1971.
49. **Watanabe Y and Uchida H.** Verapamil-induced sustained ventricular tachycardia in isolated, perfused rabbit hearts. *Jpn Circ J* 51: 188–195, 1987.
50. **Watanabe M, Otani NF, and Gilmour RF Jr.** Biphasic restitution of action potential duration and complex dynamics in ventricular myocardium. *Circ Res* 76: 915–921, 1995.
51. **Watanabe M, Zipes DP, and Gilmour RF Jr.** Oscillations of diastolic interval and refractory period following premature and postmature stimuli in canine cardiac Purkinje fibers. *PACE* 12: 1089–1103, 1989.
52. **Wu TJ, Yashima M, Doshi R, Kim YH, Athill CA, Ong JJ, Czer L, Trento A, Blanche C, Kass RM, Garfinkel A, Weiss JN, Fishbein MC, Karagueuzian HS, and Chen PS.** Relation between cellular repolarization characteristics and critical mass for human ventricular fibrillation. *J Cardiovasc Electrophysiol* 10: 1077–1086, 1999.
53. **Zipes DP and Wellens HHJ.** Sudden cardiac death. *Circulation* 98: 2334–2351, 1998.